

Boundary element analysis for the Helmholtz eigenvalue problems with a multiply connected domain

BY J. T. CHEN¹, J. H. LIN¹, S. R. KUO¹ AND S. W. CHYUAN²

¹*Department of Harbor and River Engineering, Taiwan Ocean University, Keelung, Taiwan (jtchen@mail.ntou.edu.tw)*

²*Chung-shan Institute of Science and Technology, Lung-tan, Taiwan*

Received 21 July 2000; revised 20 December 2000; accepted 14 February 2001

For a Helmholtz eigenvalue problem with a multiply connected domain, the boundary integral equation approach as well as the boundary-element method is shown to yield spurious eigenvalues even if the complex-valued kernel is used. In such a case, it is found that spurious eigenvalues depend on the geometry of the inner boundary. Demonstrated as an analytical case, the spurious eigenvalue for a multiply connected problem with its inner boundary as a circle is studied analytically. By using the degenerate kernels and circulants, an annular case can be studied analytically in a discrete system and can be treated as a special case. The proof for the general boundary instead of the circular boundary is also derived. The Burton–Miller method is employed to eliminate spurious eigenvalues in the multiply connected case. Moreover, a modified method considering only the real-part formulation is provided. Five examples are shown to demonstrate that the spurious eigenvalues depend on the shape of the inner boundary. Good agreement between analytical prediction and numerical results are found.

Keywords: boundary elements; spurious eigenvalue; degenerate kernel; circulant; multiply connected problem; Burton–Miller method

1. Introduction

It is well known that the integral equation approach results in fictitious (irregular) frequency (or wavenumber) when it is applied to solve exterior acoustic problems (Gennaretti *et al.* 1977; Schenck 1968; Schroeder & Wolff 1994; Seybert & Rengarajan 1968). The irregular values embedded in the singular (UT) and hypersingular (LM) integral equations are found to be the associated eigenvalues for the corresponding interior problem with the Dirichlet and Neumann boundary conditions, respectively (Chen 1998). To overcome this difficulty, Burton & Miller (1971) proposed an approach by adding the product of hypersingular (LM) equation with an imaginary constant to the singular (UT) equation. The other alternative is the combined Helmholtz interior integral equation formulation (CHIEF) method, which adds additional constraints by collocating the UT equation on the points in the complementary domain. The main advantage of the CHIEF method is that a hypersingular equation is not required. However, the choice of the number of points and their positions needs special attention.

For the Helmholtz eigenvalue problem with a simply connected domain, the dual reciprocity method (DRM) (Silva & Venturini 1988) and the multiple reciprocity method (MRM) (Kamiya & Andoh 1993; Nowak & Neves 1994; Nowak & Brebbia 1989) have been widely used recently. One advantage of the MRM using the Laplace-type fundamental solution is that only real-valued computation is used instead of the MRM using the Helmholtz-type fundamental solution (Itagaki & Brebbia 1993, 1994; Itagaki *et al.* 1997). It was found that the MRM is no more than the real part of the complex-valued formulation (Kamiya *et al.* 1996). A simplified method using only real-part (Tai & Shaw 1974) or imaginary-part kernels (De Mey 1976, 1977) has been presented. Also, Hutchinson (1985, 1988, 1991) replaced the complex-valued kernel by the real part only to solve the plate and membrane vibration problems. However, spurious eigenvalues occur when we use either a real-part singular or hypersingular equation. Mathematically speaking, the origin of spurious modes stems from incorrect approximation of the operator. To deal with this problem, the framework of the dual MRM (Chen *et al.* 2000*a*) and the real-part dual boundary-element method (BEM) (Kuo *et al.* 2000*a*) were constructed to filter out spurious eigenvalues. Many approaches—the residue method (Chen & Wong 1998), the domain partition technique (Chang *et al.* 1999), the generalized singular value decomposition (GSVD) (Kuo *et al.* 2000*c*), singular value decomposition (SVD) updating terms (Chen *et al.* 2000*b*; Golub & VanLoan 1989; Yeih *et al.* 1999*a, b*), SVD updating documents (Chen *et al.* 1999), the combined Helmholtz exterior integral equation formulation (CHEEF) method (Chen *et al.* 2001)—have been successfully applied to deal with the spurious solution. Based on the real-part formulation or MRM formulation using the Laplace-type fundamental solution, the spurious solutions were found only in the simply connected domain problem. However, Tai & Shaw (1974) claimed that spurious eigenvalues are not present if the complex kernel is employed. However, this point is only correct for the problem of the simply connected domain. Chang (1999) pointed out that the spurious solution is also present using the domain partition technique for the multiply connected problem, even though the complex-valued BEM was adopted to solve the eigensolution.

In this paper, the eigensolution for the multiply connected domain problem will be solved by using the complex-valued BEM. The mechanism that occurs for the spurious eigensolution in the multiply connected domain problem will be studied analytically and numerically. For the annular domain problem, the degenerate kernels for the fundamental solution and circulants resulting from circular boundary will be employed to determine the spurious solution. The factors which dominate the values of spurious eigenvalues will be discussed. To circumvent the spurious solution, the Burton–Miller method and its modified form by using only real-part information will both be used to solve the problem. Several examples will be given to demonstrate the present formulation. The results will be compared with analytical solutions if available and those of the finite-element method (FEM) using ABAQUS.

2. Mathematical analysis of the spurious eigenvalues for a multiply connected domain problem

The governing equation for an acoustic cavity is the Helmholtz equation:

$$(\nabla^2 + k^2)u(x) = 0, \quad x \in \Omega \quad (2.1)$$

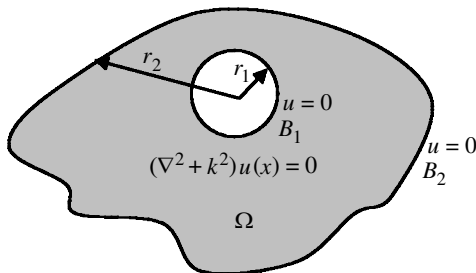


Figure 1. Helmholtz eigenvalue problem with a multiply connected domain.

where ∇^2 is the Laplace operator, Ω is the domain of the problem. Here, we consider the problem with a multiply connected region as shown in figure 1. The inner boundary is circular with radius r_1 , and the outer boundary is arbitrary and r_2 must be larger than r_1 . For simplicity, the boundary condition is assumed to be Dirichlet type: $\bar{u} = 0$ on all the boundaries. Based on the dual boundary integral formulation (Chen & Hong 1999), we have

$$\alpha u(x) = \text{CPV} \int_{B(s)} T_c(s, x)u(s) \, dB(s) - \text{RPV} \int_{B(s)} U_c(s, x)t(s) \, dB(s), \tag{2.2}$$

$$\alpha t(x) = \text{HPV} \int_{B(s)} M_c(s, x)u(s) \, dB(s) - \text{CPV} \int_{B(s)} L_c(s, x)t(s) \, dB(s), \tag{2.3}$$

where $U_c(s, x)$, $T_c(s, x)$, $L_c(s, x)$ and $M_c(s, x)$ are the kernel functions as follows,

$$U_c(s, x) = \frac{-i\pi H_0^{(1)}(kr)}{2}, \tag{2.4}$$

$$T_c(s, x) = \frac{-ik\pi}{2} H_1^{(1)}(kr) \frac{y_i n_i}{r}, \tag{2.5}$$

$$L_c(s, x) = \frac{ik\pi}{2} H_1^{(1)}(kr) \frac{y_i \bar{n}_i}{r}, \tag{2.6}$$

$$M_c(s, x) = \frac{-ik\pi}{2} \left\{ -k \frac{H_2^{(1)}(kr)}{r^2} y_i y_j n_i \bar{n}_j + \frac{H_1^{(1)}(kr)}{r} n_i \bar{n}_i \right\}, \tag{2.7}$$

in which $H_n^{(1)}(kr)$ is the n th-order Hankel function of the first kind, r is the distance between the field point x and source point s , $y_i = s_i - x_i$, $i^2 = 1$, k is the wavenumber, and n_i and \bar{n}_i are the i th components of the normal vectors at s and x , respectively, RPV, CPV and HPV denote the Riemann principal value, Cauchy principal value and Hadamard principal value, respectively, $t(s) = \partial u(s) / \partial n_s$, and α depends on the collocation point ($\alpha = 2\pi$ for an interior point, $\alpha = \pi$ for a smooth boundary point, $\alpha = 0$ for an exterior point). When the boundary is discretized into $2N$ constant elements, the linear algebraic equation can be obtained as follows,

$$[U_{ij}]_{2N \times 2N} \{t_j\}_{2N \times 1} = [T_{ij}]_{2N \times 2N} \{u_j\}_{2N \times 1}, \tag{2.8}$$

$$[L_{ij}]_{2N \times 2N} \{t_j\}_{2N \times 1} = [M_{ij}]_{2N \times 2N} \{u_j\}_{2N \times 1}, \tag{2.9}$$

where $[U_{ij}]$, $[T_{ij}]$, $[L_{ij}]$ and $[M_{ij}]$ are the four influence matrices,

$$U_{ij} = \text{RPV} \int_{B_j} U_c(s, x_i) dB(s), \quad (2.10)$$

$$T_{ij} = \text{CPV} \int_{B_j} T_c(s, x_i) dB(s) - \pi \delta_{ij}, \quad (2.11)$$

$$L_{ij} = \text{CPV} \int_{B_j} L_c(s, x_i) dB(s) + \pi \delta_{ij}, \quad (2.12)$$

$$M_{ij} = \text{HPV} \int_{B_j} M_c(s, x_i) dB(s), \quad (2.13)$$

in which $\{u_j\}$ and $\{t_j\}$ are the boundary data of the j th element.

Based on the successful experience of SVD updating terms and updating documents (Chen *et al.* 2000a, b; Kuo *et al.* 2000c), the spurious eigenvalues appear when there exists a boundary distribution $\langle \psi \rangle$ such that $\langle \psi \rangle [U] = \langle 0 \rangle$ and $\langle \psi \rangle [T] = \langle 0 \rangle$. It can be expressed in the discrete system by the row vector $\langle \psi \rangle$, which satisfies

$$\sum_{i=1}^N \psi_i U_{ij} = 0, \quad j = 1, \dots, N, \quad (2.14)$$

$$\sum_{i=1}^N \psi_i T_{ij} = 0, \quad j = 1, \dots, N. \quad (2.15)$$

When N approaches infinity for the constant element, equations (2.14) and (2.15) can be extended to continuous system as

$$\sum_{i=1}^N \psi_i U_{ij} \approx \int_{B_j(s)} dB(s) \left[\int_B \psi(x) U_c(s, x) dB(x) \right] = 0, \quad \text{for any } B_j(s), \quad (2.16)$$

$$\sum_{i=1}^N \psi_i T_{ij} \approx \int_{B_j(s)} dB(s) \left[\int_B \psi(x) T_c(s, x) dB(x) \right] = 0, \quad \text{for any } B_j(s), \quad (2.17)$$

where the boundary $B_j(s)$ can be arbitrarily chosen. The spurious eigenvalues appear when

$$\int_B \psi(x) U_c(s, x) dB(x) = 0, \quad \text{for any } s, \quad (2.18)$$

$$\int_B \psi(x) T_c(s, x) dB(x) = 0, \quad \text{for any } s. \quad (2.19)$$

Equations (2.18) and (2.19) indicate that the null field ($u = 0$ and $t = 0$) exists when the singularity distribution ψ is superimposed on the boundary.

Now a multiply connected domain with an inner boundary of a circle is considered as shown in figure 1. We choose a specific $\psi_n(x)$, $n = 0, 1, 2, \dots$, as follows,

$$\psi_n(x) = \cos(n\theta), \quad x \text{ on the inner boundary } B_1, \quad (2.20)$$

$$\psi_n(x) = 0, \quad x \text{ on the outer boundary } B_2, \quad (2.21)$$

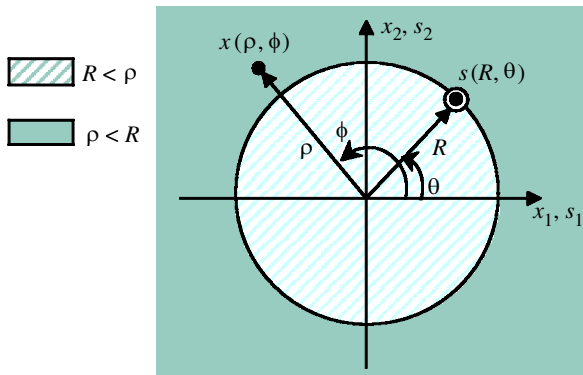


Figure 2. Symbols for the degenerate kernels.

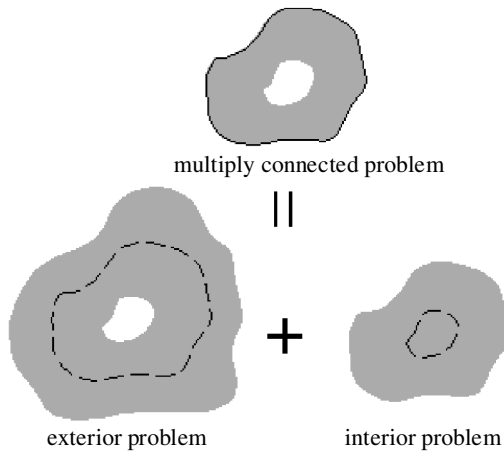


Figure 3. Decomposition of a multiply connected problem.

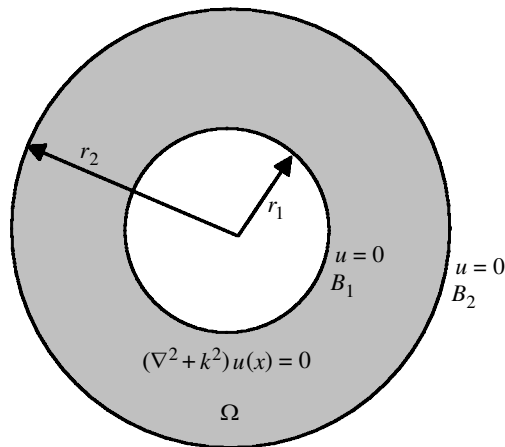


Figure 4. Helmholtz eigenvalue problem with an annular domain.

and the complex degenerate kernels in the dual formulation are

$$U_c(s, x) = \begin{cases} U^i(s, x) = \sum_{m=-\infty}^{\infty} \frac{1}{2} \pi J_m(k\rho) (Y_m(kR) - iJ_m(kR)) \cos(m(\theta - \phi)), & R > \rho, \\ U^e(s, x) = \sum_{m=-\infty}^{\infty} \frac{1}{2} \pi J_m(kR) (Y_m(k\rho) - iJ_m(k\rho)) \cos(m(\theta - \phi)), & \rho > R, \end{cases} \quad (2.22)$$

$$T_c(s, x) = \begin{cases} T^i(s, x) = \sum_{m=-\infty}^{\infty} \frac{1}{2} \pi k J'_m(k\rho) (Y'_m(kR) - iJ'_m(kR)) \cos(m(\theta - \phi)), & R > \rho, \\ T^e(s, x) = \sum_{m=-\infty}^{\infty} \frac{1}{2} \pi k J'_m(kR) (Y_m(k\rho) - iJ_m(k\rho)) \cos(m(\theta - \phi)), & \rho > R, \end{cases} \quad (2.23)$$

$$L_c(s, x) = \begin{cases} L^i(s, x) = \sum_{m=-\infty}^{\infty} \frac{1}{2} \pi k J'_m(k\rho) (Y_m(kR) - iJ_m(kR)) \cos(m(\theta - \phi)), & R > \rho, \\ L^e(s, x) = \sum_{m=-\infty}^{\infty} \frac{1}{2} \pi k J_m(kR) (Y'_m(k\rho) - iJ'_m(k\rho)) \cos(m(\theta - \phi)), & \rho > R, \end{cases} \quad (2.24)$$

$$M_c(s, x) = \begin{cases} M^i(s, x) = \sum_{m=-\infty}^{\infty} \frac{1}{2} \pi k^2 J'_m(k\rho) (Y'_m(kR) - iJ'_m(kR)) \cos(m(\theta - \phi)), & R > \rho, \\ M^e(s, x) = \sum_{m=-\infty}^{\infty} \frac{1}{2} \pi k^2 J'_m(kR) (Y'_m(k\rho) - iJ'_m(k\rho)) \cos(m(\theta - \phi)), & \rho > R, \end{cases} \quad (2.25)$$

where the superscripts 'i' and 'e' denote the interior point ($R > \rho$) and the exterior point ($R < \rho$), respectively, $x = (\rho, \phi)$ and $s = (R, \theta)$ in the polar coordinate as shown in figure 2. Substituting equations (2.20)–(2.23) into (2.18) and (2.19), we have

$$\begin{aligned} \int_B \psi(x) U_c(s, x) dB(x) &= \int_{B_1(x)} (\cos n\theta) U_c(s_1, x) r_1 d\theta + \int_{B_1(x)} (\cos n\theta) U_c(s_2, x) r_1 d\theta \\ &= \pi^2 r_1 J_n(kr_1) \{ [Y_n(kr_1) + Y_n(kr_2)] - i [J_n(kr_1) + J_n(kr_2)] \} \end{aligned} \quad (2.26)$$

and

$$\begin{aligned} \int_B \psi(x) T_c(s, x) dB(x) &= \int_{B_1(x)} (\cos n\theta) T_c(s_1, x) r_1 d\theta + \int_{B_1(x)} (\cos n\theta) T_c(s_2, x) r_1 d\theta \\ &= \pi^2 r_1 J_n(kr_1) \{ [Y'_n(kr_1) + Y'_n(kr_2)] - i [J'_n(kr_1) + J'_n(kr_2)] \}, \end{aligned} \quad (2.27)$$

where s_1 and s_2 denote inner and outer boundaries, respectively.

Table 1. True and spurious eigenequations of the Helmholtz eigenvalue problem with an annular domain
 (U_r and L_r are the real parts of the U_c and L_c kernels, respectively.)

fundamental solution	true eigenequation	spurious eigenequation	non-zero term
$U_c(s, x)$	$J_n(ka)Y_n(kb) - J_n(kb)Y_n(ka) = 0$	$J_n(kb) = 0$	$Y_n(ka) - iJ_n(ka) \neq 0$
$L_c(s, x)$	$J_n(ka)Y_n(kb) - J_n(kb)Y_n(ka) = 0$	$J'_n(kb) = 0$	$Y'_n(ka) - iJ'_n(ka) \neq 0$
$ik[U_c(s, x)] + [L_c(s, x)]$	$J_n(ka)Y_n(kb) - J_n(kb)Y_n(ka) = 0$	none	$[J_n^2(kb) + J_n^2(kb)] \times \{[J_n(ka) - Y'_n(ka)]^2 + [J'_n(ka) + Y_n(ka)]^2\} \neq 0$
$ik[U_r(s, x)] + [L_r(s, x)]$	$J_n(ka)Y_n(kb) - J_n(kb)Y_n(ka) = 0$	none	$[J_n^2(kb) + J_n^2(kb)][Y_n^2(ka) + Y_n^2(ka)] \neq 0$
$k[U_r(s, x)] + [L_r(s, x)]$	$J_n(ka)Y_n(kb) - J_n(kb)Y_n(ka) = 0$	$J_n(kb) + J'_n(kb) = 0$ $Y_n(kb) + Y'_n(kb) = 0$	

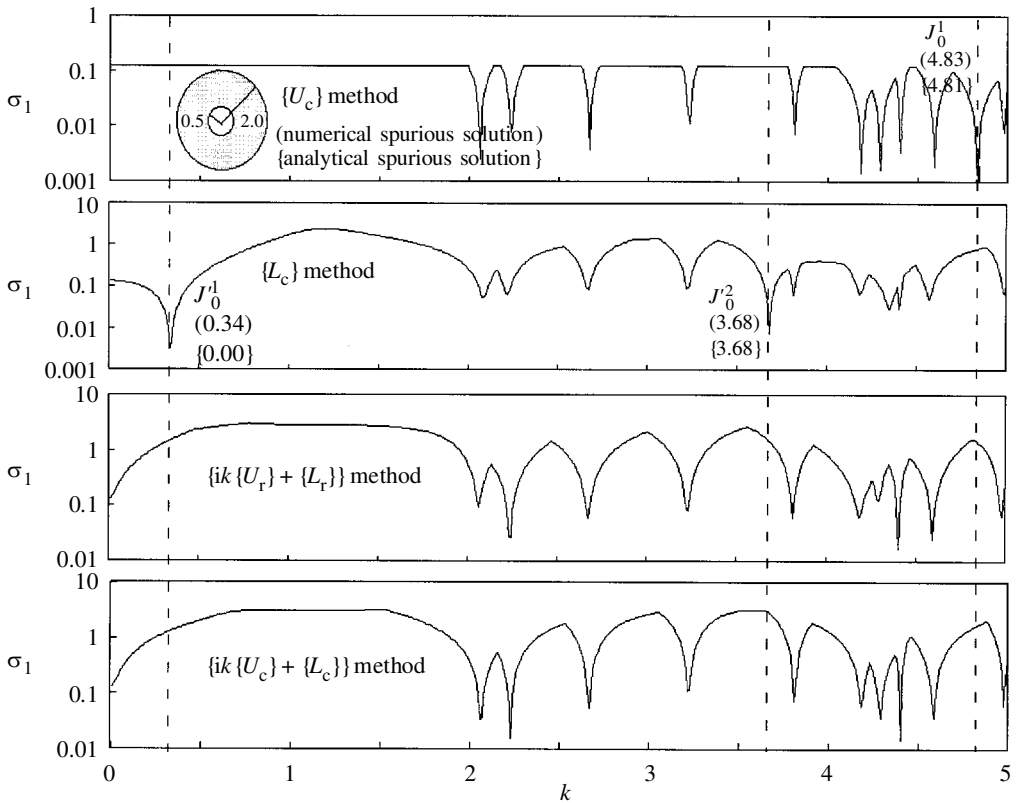


Figure 5. The minimum singular value σ_1 versus k using different approaches for the Dirichlet problem ($u = 0$) with an annular domain.

Comparing equation (2.26) with equation (2.27), we find that the spurious eigen-equation using the complex-valued singular integral equation (UT formulation) is

$$J_n(kr_1) = 0, \quad n = 0, \pm 1, \pm 2, \dots \tag{2.28}$$

Similarly, we can derive the spurious eigenequation as follows,

$$J'_n(kr_1) = 0, \quad n = 0, \pm 1, \pm 2, \dots, \tag{2.29}$$

if the hypersingular equation (LM formulation) is used. However, when we use the fundamental solution, $ikU_c(s, x) + L_c(s, x)$ (Burton–Miller method) or $ik[U_r(s, x)] + [L_r(s, x)]$ (modified method), the spurious eigenvalues will be suppressed, since the spurious eigenequations have no solution for any values of k . According to the above proof, the spurious eigenvalues depend on the inner boundary. One can understand that the multiply connected domain problem can be superimposed by two problems, one interior problem and one exterior problem, as shown in figure 3. The source which causes the spurious eigenvalues stems from the exterior problem with the inner boundary, since it is well known that fictitious (spurious) frequency is inherent in the integral formulation even though the complex kernel (UT or LM equation) is employed.

Table 2. Zeros of Bessel functions for $J_n(k)$ and $J'_n(k)$

	1	2	3	4	5
$J_0(k) = 0$	2.4048	5.5201	8.6537	11.7915	14.9309
$J_1(k) = 0$	3.83171	7.01559	10.17346	13.3237	16.4706
$J_2(k) = 0$	5.1356	8.4172	11.6198	14.7960	17.9598
$J_3(k) = 0$	6.38016	9.76102	13.0152	16.22346	19.40941
$J_4(k) = 0$	7.58834	11.0647	14.3725	17.6160	20.8269
$J_5(k) = 0$	8.77148	12.3386	15.7002	18.9801	22.2178
$J'_0(k) = 0$	0	3.83171	7.01559	10.17346	13.3237
$J'_1(k) = 0$	1.84118	5.33144	8.53632	11.70600	14.8636
$J'_2(k) = 0$	3.05424	6.70713	9.96947	13.17037	16.3475
$J'_3(k) = 0$	4.20119	8.01524	11.3459	14.5858	17.7887
$J'_4(k) = 0$	5.31755	9.2824	12.6819	15.9641	19.1960
$J'_5(k) = 0$	6.41562	10.5199	13.9872	17.3128	20.5755

3. Special case, an annular problem

We considered an annular domain problem with the Dirichlet-type boundary condition as shown in figure 4. The dual boundary integral equations can be derived as follows:

$$\int_{B_1} U_c(s, x_1) t_1(s) dB(s) + \int_{B_2} U_c(s, x_1) t_2(s) dB(s) = 0, \quad x_1 \text{ on } B_1(r_1^-), \quad (3.1)$$

$$\int_{B_1} U_c(s, x_2) t_1(s) dB(s) + \int_{B_2} U_c(s, x_2) t_2(s) dB(s) = 0, \quad x_2 \text{ on } B_2(r_2^+) \quad (3.2)$$

and

$$\int_{B_1} L_c(s, x_1) t_1(s) dB(s) + \int_{B_2} L_c(s, x_1) t_2(s) dB(s) = 0, \quad x_1 \text{ on } B_1(r_1^-) \quad (3.3)$$

$$\int_{B_1} L_c(s, x_2) t_1(s) dB(s) + \int_{B_2} L_c(s, x_2) t_2(s) dB(s) = 0, \quad x_2 \text{ on } B_2(r_2^+), \quad (3.4)$$

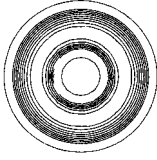
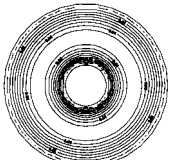
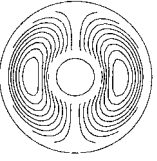
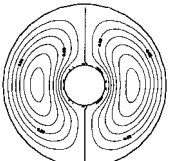
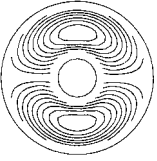
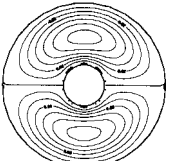
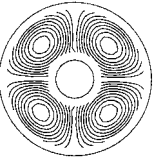
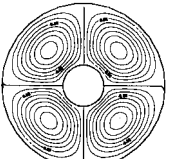
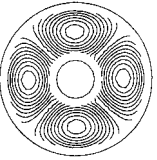
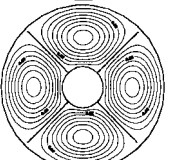
where B_1 is the inner circular boundary and B_2 is the outer circular boundary. The collocation points of r_1^- and r_2^+ are designed to avoid the source terms in the domain. Discretizing the interior and exterior circles into $2N$ constant elements, respectively, we can obtain the linear algebraic dual equations:

$$\begin{bmatrix} U_{11} & U_{12} \\ U_{21} & U_{22} \end{bmatrix}_{4N \times 4N} \begin{Bmatrix} t_1 \\ t_2 \end{Bmatrix}_{4N \times 1} = \begin{Bmatrix} 0 \\ 0 \end{Bmatrix}_{4N \times 1} \quad (3.5)$$

and

$$\begin{bmatrix} L_{11} & L_{12} \\ L_{21} & L_{22} \end{bmatrix}_{4N \times 4N} \begin{Bmatrix} t_1 \\ t_2 \end{Bmatrix}_{4N \times 1} = \begin{Bmatrix} 0 \\ 0 \end{Bmatrix}_{4N \times 1}, \quad (3.6)$$

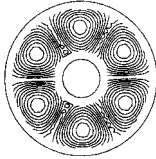
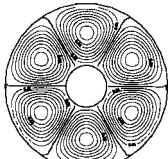
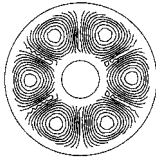
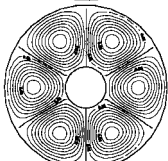
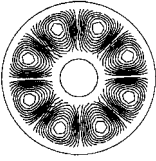
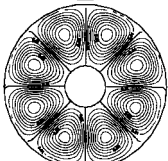
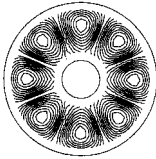
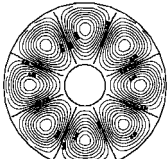
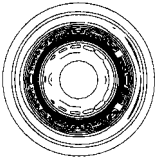
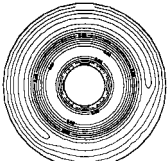
Table 3. *The first ten eigenvalues and eigenmodes of the Helmholtz eigenvalue problem with an annular domain by different approaches*

mode	eigenvalue (FEM)	mode shape (FEM)	eigenvalue (BEM)	mode shape (BEM)
1	2.03		2.06	
2	2.20		2.23	
3	2.20		2.23	
4	2.62		2.67	
5	2.62		2.67	

where the subscripts ‘1’ and ‘2’ in the submatrices of U or L and $\{u\}$ or $\{t\}$ vectors denote the positions of quantities on the inner and outer boundary, respectively. Based on the circular symmetry, the influence matrices for the discrete system are found to be circulants with the following forms (Chen *et al.* 1999; Chen & Kuo 2000; Davis 1979; Goldberg 1991; Kuo *et al.* 2000*a, b*):

$$[U_{11}] = \begin{bmatrix} u_0 & u_1 & u_2 & \cdots & u_{2N-1} \\ u_{2N-1} & u_0 & u_1 & \cdots & u_{2N-2} \\ u_{2N-2} & u_{2N-1} & u_0 & \cdots & u_{2N-3} \\ \vdots & \vdots & \vdots & \ddots & \vdots \\ u_1 & u_2 & u_3 & \cdots & u_0 \end{bmatrix}_{2N \times 2N} \quad (3.7)$$

Table 3. *Cont.*

mode	eigenvalue (FEM)	mode shape (FEM)	eigenvalue (BEM)	mode shape (BEM)
6	3.15		3.22	
7	3.15		3.22	
8	3.71		3.81	
9	3.71		3.81	
10	4.06		4.18	

If the degenerate kernel in equation (2.22) is used, the elements in the matrix $[U_{11}]$ of equation (3.7) can be obtained by

$$u_m = \int_{(m-(1/2))\Delta\theta}^{(m+(1/2))\Delta\theta} U^i(R, \theta; \rho, \phi) \rho \, d\theta \approx U^i(R, \theta_m; \rho, \phi) \rho \Delta\theta, \quad m = 0, 1, 2, \dots, 2N - 1, \quad (3.8)$$

where $\Delta\theta = 2\pi/2N$ and $\theta_m = m\Delta\theta$.

By introducing the following bases for circulants, I ,

$$(C_{2N})^1, (C_{2N})^2, \dots, (C_{2N})^{2N-1},$$

we can expand matrix $[U_{11}]$ into

$$[U_{11}] = u_0 I + u_1 (C_{2N})^1 + u_2 (C_{2N})^2 + \dots + u_{2N-1} (C_{2N})^{2N-1}, \quad (3.9)$$

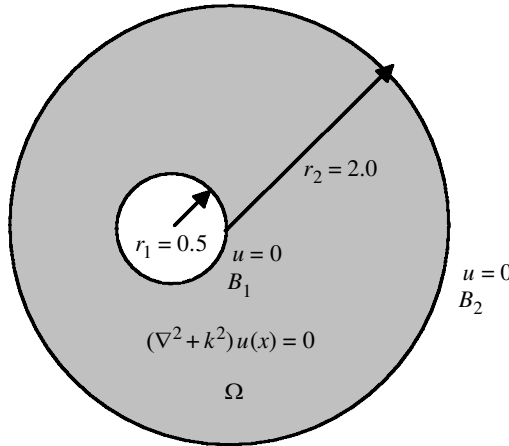


Figure 6. Helmholtz eigenvalue problem with an eccentric domain.

where

$$C_{2N} = \begin{bmatrix} 0 & 1 & 0 & \cdots & 0 \\ 0 & 0 & 1 & \cdots & 0 \\ 0 & 0 & 0 & \cdots & 0 \\ \vdots & \vdots & \vdots & \ddots & \vdots \\ 1 & 0 & 0 & \cdots & 0 \end{bmatrix}_{2N \times 2N} \quad (3.10)$$

Based on the similar properties for the matrices of $[U_{11}]$ and $[C_N]$, we have

$$\lambda_l^{[U_{11}]} = u_0 + u_1\alpha_l + u_2\alpha_l^2 + \cdots + u_{2N-1}\alpha_l^{2N-1}, \quad l = 0, 1, 2, \dots, 2N - 1, \quad (3.11)$$

where $\lambda_l^{[U_{11}]}$ and α_l are the eigenvalues for $[U]$ and $[C_N]$, respectively. It is easily found that the eigenvalues and eigenvectors for the circulants $[C_{2N}]$ are the roots for $\alpha^{2N} = 1$, as shown below:

$$\alpha_l = e^{i(2\pi l/2N)}, \quad l = 0, 1, 2, \dots, 2N - 1, \quad (3.12)$$

$$\{\phi_l\} = \left\{ \begin{matrix} 1 \\ \alpha_l \\ \alpha_l^2 \\ \vdots \\ \alpha_l^{2N-1} \end{matrix} \right\}_{2N}, \quad (3.13)$$

respectively. Substituting equation (3.12) into equation (3.11), we have

$$\begin{aligned} \lambda_l^{[U_{11}]} &= \sum_{m=0}^{2N-1} u_m(\alpha_l)^m = \sum_{m=0}^{2N-1} u_m e^{iml(2\pi/2N)} \\ &= \sum_{m=0}^{2N-1} U^e(r_1, \theta; r_1, \phi) r_1 \Delta\theta e^{iml\Delta\theta} = r_1 \sum_{m=0}^{2N-1} U^e(r_1, \theta; r_1, \phi) e^{iml\Delta\theta} \Delta\theta. \end{aligned} \quad (3.14)$$

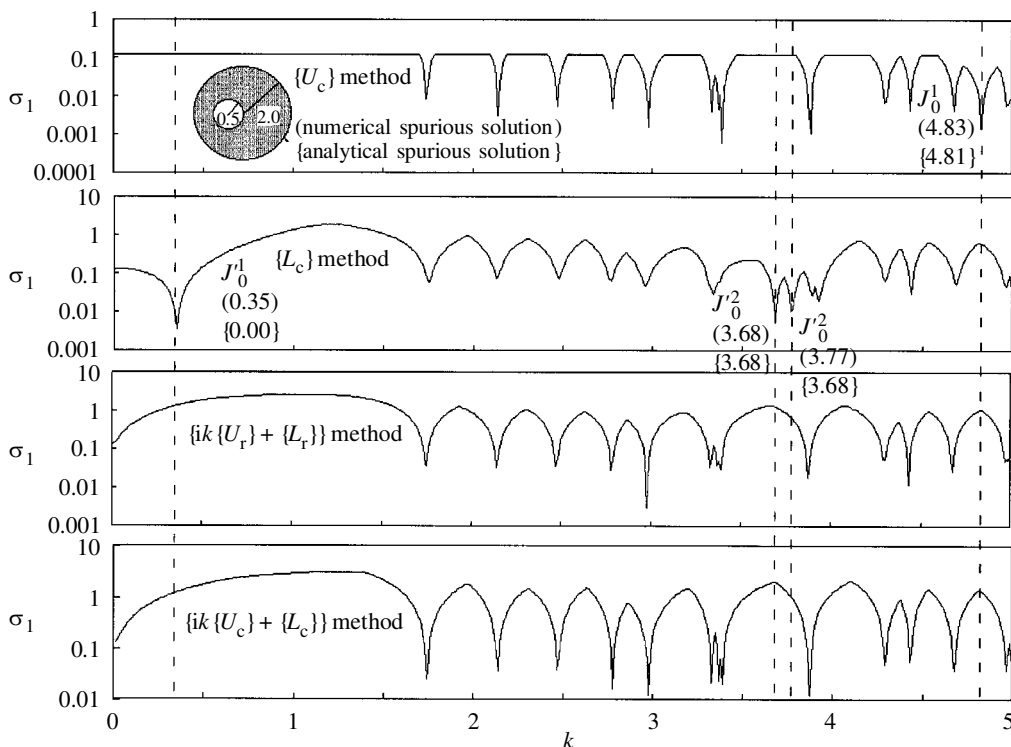


Figure 7. The minimum singular value σ_1 versus k using different approaches for the Dirichlet problem ($u = 0$) with an eccentric domain.

Table 4. The first ten eigenvalues of Helmholtz eigenvalue problem with an eccentric domain

	1	2	3	4	5	6	7	8	9	10
FEM	1.73	2.13	2.45	2.76	2.95	3.30	3.34	3.36	3.83	3.84
Chen & Zhou (1992)	1.75	2.14	2.47	2.78	2.97	3.33	3.37	3.38	3.85	3.87
Burton & Miller (1971)	1.74	2.14	2.47	2.78	2.98	3.33	3.37	3.39	3.87	3.87
modified Burton–Miller	1.75	2.14	2.47	2.78	2.98	3.33	3.37	3.39	3.87	3.87

When N approaches infinity, the Riemann sum in equation (3.14) can be transformed to the following integral:

$$\lambda_l^{[U_{11}]} = r_1 \int_0^{2\pi} U^e(r_1, \theta; r_1, \phi) e^{i l \theta} d\theta. \tag{3.15}$$

By substituting the U^i kernel of equation (2.22) into equation (3.15), we have

$$\begin{aligned} \lambda_l^{[U_{11}]} &= r_1 \int_0^{2\pi} \left(\sum_{m=-\infty}^{\infty} \frac{1}{2} \pi J_m(k\rho) \left(Y_m(kR) - iJ_m(kR) \right) \cos(m(\theta - \phi)) \right) e^{i l \theta} d\theta \\ &= \pi^2 r_1 J_l(kr_1) (Y_l(kr_1) - iJ_l(kr_1)), \quad l = 0, \pm 1, \pm 2, \dots, \pm(N - 1), N. \end{aligned} \tag{3.16}$$

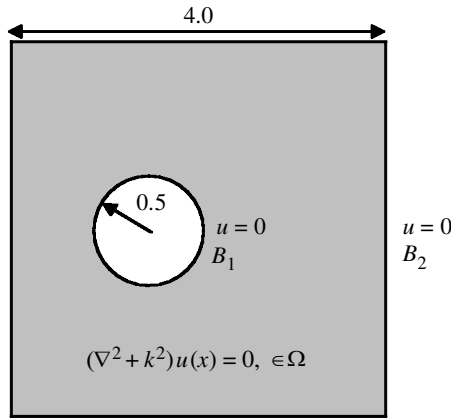


Figure 8. Helmholtz eigenvalue problem with an inner circular and outer square domain.

Similarly, we can obtain the eigenvalues for the other influence matrices:

$$\lambda_l^{[U_{12}]} = \pi^2 r_2 J_l(kr_1)(Y_l(kr_2) - iJ_l(kr_2)), \quad l = 0, \pm 1, \pm 2, \dots, \pm(N - 1), N. \quad (3.17)$$

$$\lambda_l^{[U_{21}]} = \pi^2 r_1 J_l(kr_1)(Y_l(kr_2) - iJ_l(kr_2)), \quad l = 0, \pm 1, \pm 2, \dots, \pm(N - 1), N. \quad (3.18)$$

$$\lambda_l^{[U_{22}]} = \pi^2 r_2 J_l(kr_2)(Y_l(kr_2) - iJ_l(kr_2)), \quad l = 0, \pm 1, \pm 2, \dots, \pm(N - 1), N. \quad (3.19)$$

$$\lambda_l^{[L_{11}]} = \pi^2 kr_1 J'_l(kr_1)(Y_l(kr_1) - iJ_l(kr_1)), \quad l = 0, \pm 1, \pm 2, \dots, \pm(N - 1), N. \quad (3.20)$$

$$\lambda_l^{[L_{12}]} = \pi^2 kr_2 J'_l(kr_1)(Y_l(kr_2) - iJ_l(kr_2)), \quad l = 0, \pm 1, \pm 2, \dots, \pm(N - 1), N. \quad (3.21)$$

$$\lambda_l^{[L_{21}]} = \pi^2 kr_1 J_l(kr_1)(Y'_l(kr_2) - iJ'_l(kr_2)), \quad l = 0, \pm 1, \pm 2, \dots, \pm(N - 1), N. \quad (3.22)$$

$$\lambda_l^{[L_{22}]} = \pi^2 kr_2 J_l(kr_2)(Y'_l(kr_2) - iJ'_l(kr_2)), \quad l = 0, \pm 1, \pm 2, \dots, \pm(N - 1), N. \quad (3.23)$$

In order to calculate the determinant, we can decompose the circulants U_{ij} and L_{ij} into

$$[U_{ij}] = [\Phi][\bar{U}_{ij}][\Phi]^*, \quad (3.24)$$

$$[L_{ij}] = [\Phi][\bar{L}_{ij}][\Phi]^*, \quad (3.25)$$

where $[\Phi]$ is a unitary matrix composed of $\{\phi_l\}$ vectors in equation (3.13) and $[\Phi]^*$ is the conjugate transpose of $[\Phi]$, the elements in the diagonal matrices $[\bar{U}_{ij}]$ and $[\bar{L}_{ij}]$ are the eigenvalues of the $[U_{ij}]$ and $[L_{ij}]$. Then the determinant of the matrix

$$\begin{bmatrix} U_{11} & U_{12} \\ U_{21} & U_{22} \end{bmatrix}$$

is

$$\begin{aligned} \det \left[\begin{bmatrix} U_{11} & U_{12} \\ U_{21} & U_{22} \end{bmatrix} \right] &= \det \begin{bmatrix} \bar{U}_{11} & \bar{U}_{12} \\ \bar{U}_{21} & \bar{U}_{22} \end{bmatrix} \cdot \det |[\Phi]^*[\Phi]| \\ &= \det \begin{bmatrix} \bar{U}_{11} & \bar{U}_{12} \\ \bar{U}_{21} & \bar{U}_{22} \end{bmatrix} = \prod_{l=-N+1}^N \det \begin{bmatrix} \lambda_l^{[U_{11}]} & \lambda_l^{[U_{12}]} \\ \lambda_l^{[U_{21}]} & \lambda_l^{[U_{22}]} \end{bmatrix}. \end{aligned} \quad (3.26)$$

Similarly, we have

$$\det \begin{bmatrix} L_{11} & L_{12} \\ L_{21} & L_{22} \end{bmatrix} = \prod_{l=-N+1}^N \det \begin{bmatrix} \lambda_l^{[L_{11}]} & \lambda_l^{[L_{12}]} \\ \lambda_l^{[L_{21}]} & \lambda_l^{[L_{22}]} \end{bmatrix}, \quad (3.27)$$

Equations (3.26) and (3.27) can be simplified to

$$\det \begin{bmatrix} U_{11} & U_{12} \\ U_{21} & U_{22} \end{bmatrix} = \prod_{l=0}^N \lambda_l^U \prod_{l=1}^{N-1} \lambda_l^U, \quad (3.28)$$

and

$$\det \begin{bmatrix} L_{11} & L_{12} \\ L_{21} & L_{22} \end{bmatrix} = \prod_{l=0}^N \lambda_l^L \prod_{l=1}^{N-1} \lambda_l^L, \quad (3.29)$$

where

$$\lambda_l^U = \pi^4 r_1 r_2 J_l(kr_1) [J_l(kr_2) Y_l(kr_1) - J_l(kr_1) Y_l(kr_2)] [Y_l(kr_2) - iJ(kr_2)], \quad (3.30)$$

$$\lambda_l^L = \pi^4 k^2 r_1 r_2 J_l'(kr_1) [J_l(kr_2) Y_l(kr_1) - J_l(kr_1) Y_l(kr_2)] [Y_l'(kr_2) - iJ'(kr_2)]. \quad (3.31)$$

From equations (3.28) and (3.29), we can obtain the possible eigenequations

$$\begin{aligned} J_l(kr_1) = 0, \quad J_l(kr_2) Y_l(kr_1) - J_l(kr_1) Y_l(kr_2) = 0, \\ Y_l(kr_2) - iJ(kr_2) = 0 \quad (\text{UT equation}), \end{aligned} \quad (3.32)$$

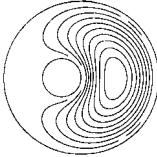
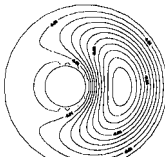

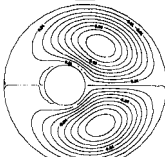
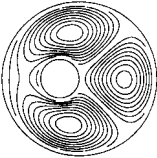
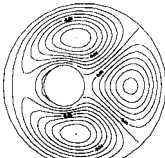
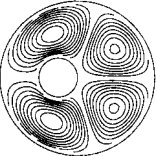
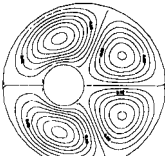
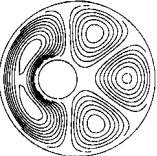

$$\begin{aligned} J_l'(kr_1) = 0, \quad J_l(kr_2) Y_l(kr_1) - J_l(kr_1) Y_l(kr_2) = 0, \\ Y_l'(kr_2) - iJ'(kr_2) = 0 \quad (\text{LM equation}). \end{aligned} \quad (3.33)$$

Comparing equation (3.32) with equation (3.33), we find that the true eigenvalues occur when $J_l(kr_2) Y_l(kr_1) - J_l(kr_1) Y_l(kr_2) = 0$, and the spurious eigenvalues occur when $J_l(kr_1) = 0$ or $J_l'(kr_1) = 0$, since $Y_l(kr_2) - iJ(kr_2)$ and $Y_l'(kr_2) - iJ'(kr_2)$ are never zeros for any value of k . Similarly, we can obtain the true eigenequations without spurious contamination when the fundamental solution is chosen as $ik[U_c(s, x)] + L_c(s, x)$ or using only the real-part kernel, $ik[U_r(s, x)] + L_r(s, x)$. Table 1 shows the true and spurious eigenequations occurring in the different methods using various fundamental solutions.

4. Numerical examples for Helmholtz eigenvalue problem with a multiply connected domain

We consider five cases of Helmholtz eigenvalue problems with a multiply connected domain subjected to the Dirichlet boundary condition. The fundamental solutions we used are the complex $U_c(s, x)$ kernel, complex $L_c(s, x)$ kernel, $ik[U_c(s, x)] + L_c(s, x)$ (Burton–Miller method) and $ik[U_r(s, x)] + L_r(s, x)$ (modified method). The SVD technique is employed to examine the singularity of the coefficient matrix in order to find the eigenvalues and eigenmodes.

Table 5. *The first ten eigenvalues and eigenmodes of the Helmholtz eigenvalue problem with an eccentric domain by different approaches*

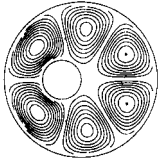
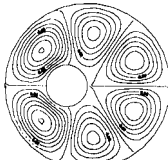
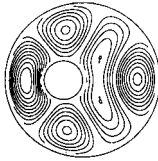
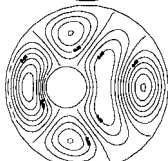
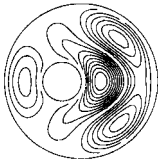
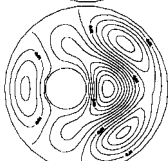
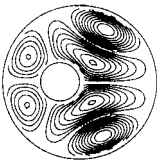
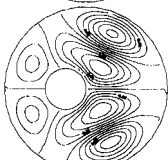

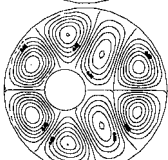
mode	eigenvalue (FEM)	mode shape (FEM)	eigenvalue (BEM)	mode shape (BEM)
1	1.74		1.74	
2	2.13		2.14	
3	2.45		2.47	
4	2.76		2.78	
5	2.95		2.97	

Case 1: an annular case. An annular domain is considered in figure 4. The radii of inner and outer circular boundaries are 0.5 and 2.0, respectively. Figure 5 shows the minimum singular value σ_1 versus k using four approaches: $[U_c]$ method using $[U_c]$ kernel, $[L_c]$ method using $[L_c]$ kernel, real-part Burton–Miller method using $ik[U_r] + [L_r]$ kernel, and Burton–Miller method using $ik[U_c] + [L_c]$ kernel. We find that the spurious eigenvalues occur as predicted theoretically when one of the complex-valued kernels $U_c(s, x)$ ($[U_c]$ method) or $L_c(s, x)$ ($[L_c]$ method) is used. The common dips for the four methods are the true eigenvalues; otherwise, the dips are spurious. The spurious eigenvalues can be suppressed by using the Burton–Miller method ($ik[U_c(s, x)] + L_c(s, x)$ method) or modified Burton–Miller method ($ik[U_r(s, x)] + L_r(s, x)$ method).

When the complex-valued kernel $U_c(s, x)$ was used, the spurious eigenvalues occur when k satisfies

$$J_n(0.5k) = 0, \quad n = 0, \pm 1, \pm 2, \dots, \pm(N - 1), N. \tag{4.1}$$

Table 5. *Cont.*

mode	eigenvalue (FEM)	mode shape (FEM)	eigenvalue (BEM)	mode shape (BEM)
6	3.30		3.33	
7	3.34		3.37	
8	3.36		3.37	
9	3.83		3.87	
10	3.84		3.87	

When the complex-valued kernel $L_c(s, x)$ was used, the spurious eigenvalues occur when k satisfies

$$J'_n(0.5k) = 0, \quad n = 0, \pm 1, \pm 2, \dots, \pm(N-1), N. \quad (4.2)$$

The spurious eigenvalues can be obtained from table 2. The first ten eigenvalues and eigenmodes using BEM and FEM are shown in table 3. In figure 5, good agreement between analytical prediction and numerical results for spurious eigenvalues is found.

Case 2: an eccentric case. An eccentric case is considered in figure 6 and the radii of inner and outer circular boundaries are 0.5 and 2.0, respectively. Figure 7 shows the minimum singular value σ_1 versus k using different approaches. We find that the spurious eigenvalues occur when one of the complex-valued kernels $U_c(s, x)$ or $L_c(s, x)$ was used in a similar way to figure 5. The spurious eigenvalues can be filtered out by using the $ik[U_c(s, x)] + L_c(s, x)$ kernel (the Burton–Miller method) or $ik[U_r(s, x)] + L_r(s, x)$ kernel (modified Burton–Miller method). The true eigenvalues

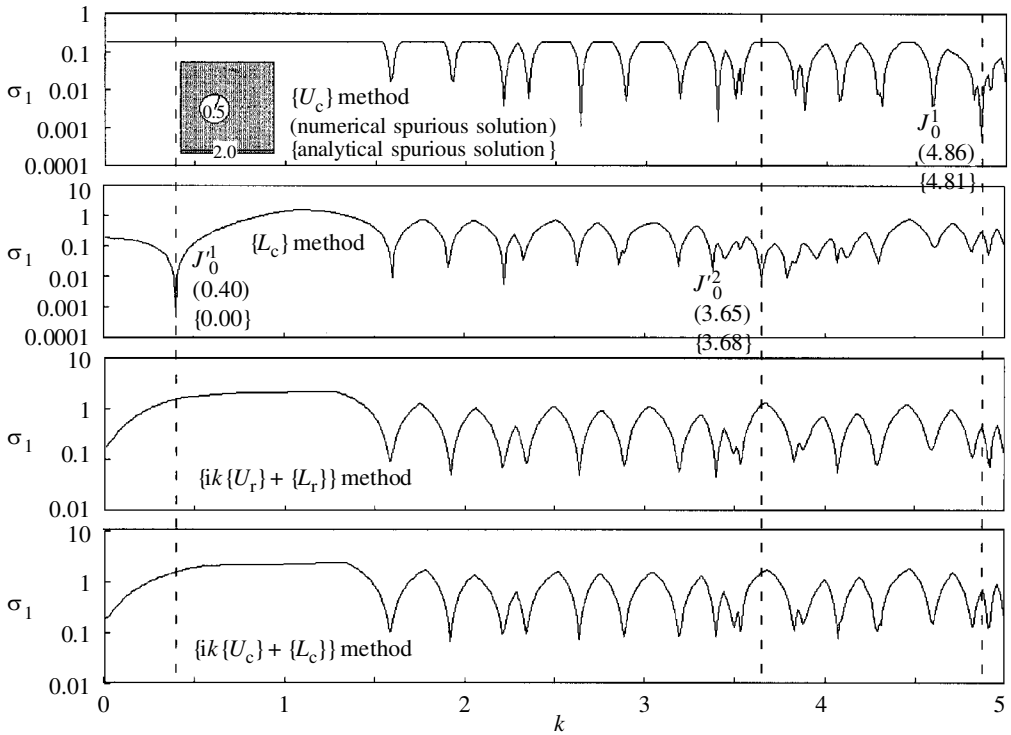


Figure 9. The minimum singular value σ_1 versus k using different approaches for the Dirichlet problem ($u = 0$) with an inner circular and outer square domain.

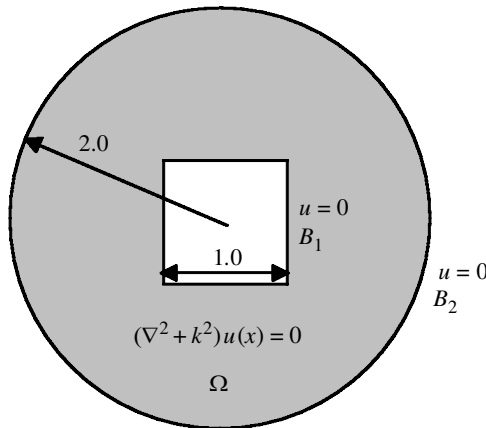


Figure 10. Helmholtz eigenvalue problem with an inner square and outer circular domain.

are compared with the results by using FEM and BEM by Chen & Zhou (1992) in table 4. The first ten modes by using BEM and FEM are shown in table 5. Since the complex-valued kernel $U_c(s, x)$ was used, the spurious eigenvalues occur when k satisfies

$$J_n(0.5k) = 0, \quad n = 0, \pm 1, \pm 2, \dots \tag{4.3}$$

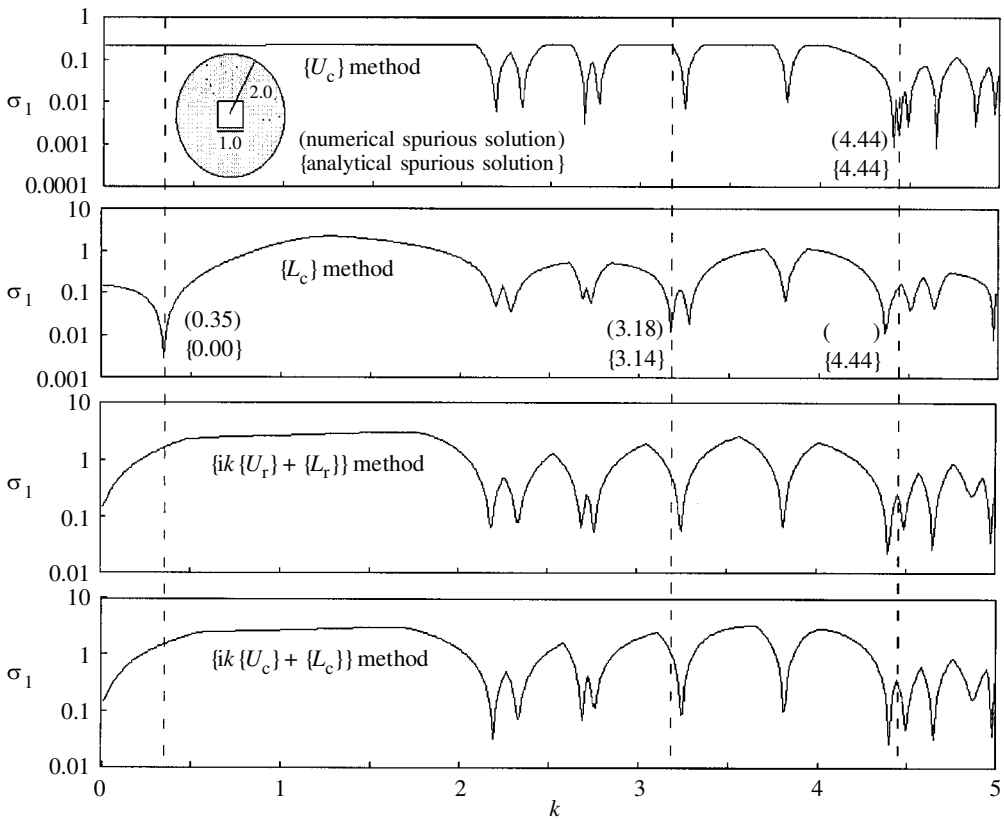


Figure 11. The minimum singular value σ_1 versus k using different approaches for the Dirichlet problem ($u = 0$) with an inner square domain.

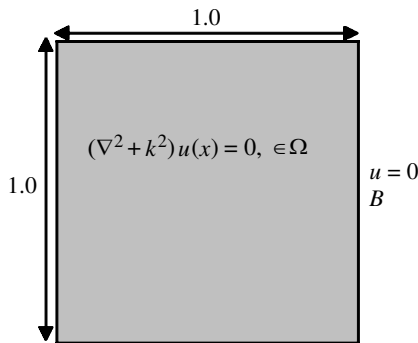


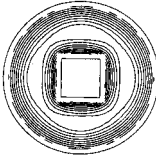
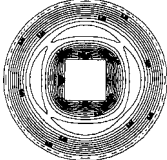
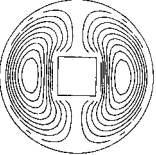
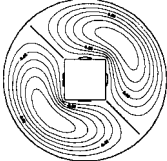
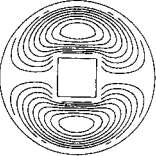
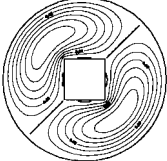
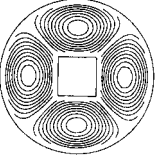
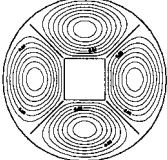
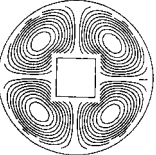
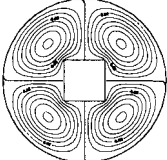
Figure 12. Helmholtz eigenvalue problem with a square domain.

Similarly, the spurious eigenvalues occur when k satisfies

$$J'_n(0.5k) = 0, \quad n = 0, \pm 1, \pm 2, \dots \tag{4.4}$$

if the complex-valued kernel $L_c(s, x)$ is adopted. The spurious eigenvalues match very well the analytical solutions in equations (4.3) and (4.4). The true solutions between FEM and BEM agree very well.

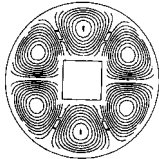
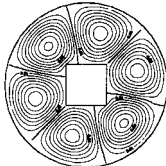
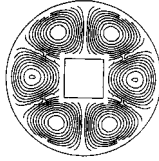
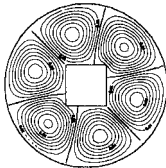
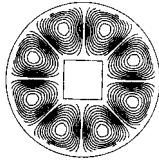
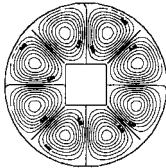

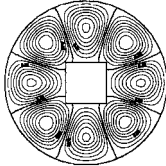

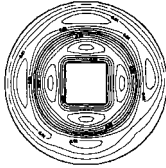
Table 6. The first ten eigenvalues and eigenmodes of the Helmholtz eigenvalue problem with an inner square and outer circular domain (I) by different approaches

mode	eigenvalue (FEM)	mode shape (FEM)	eigenvalue (BEM)	mode shape (BEM)
1	2.19		2.19	
2	2.33		2.33	
3	2.33		2.33	
4	2.67		2.69	
5	2.76		2.76	

Case 3: inner circle and outer square. In this case we considered the multiply connected problem with an inner boundary of a circle and an outer boundary of a square, as shown in figure 8. In figure 9 we found that the minimum singular value drops at the positions of the spurious eigenvalues which are the same locations of cases 1 and 2. This numerical experiment indicates that the spurious eigensolution is dominated by the inner boundary and is independent of the shape of the outer boundary, as predicted theoretically.

Case 4: inner square and outer circle (I). A multiply connected domain composed of an inner square boundary and outer circular boundary is considered in figure 10. Figure 11 also shows the minimum singular value σ_1 versus k by using four approaches. The first ten eigenvalues and eigenmodes by BEM and FEM are shown in table 6. We expect that the position of spurious eigenvalues is associated with the interior natural frequency with essential or natural homogeneous boundary conditions. The analytical solution of the eigenvalues for an interior acoustic problem

Table 6. *Cont.*

mode	eigenvalue (FEM)	mode shape (FEM)	eigenvalue (BEM)	mode shape (BEM)
6	3.22		3.24	
7	3.22		3.24	
8	3.76		3.81	
9	3.77		3.81	
10	4.32		4.40	

with a square domain in figure 12 is

$$k_{mn} = \pi \sqrt{m^2 + n^2} \quad (m, n = 1, 2, 3, \dots),$$

homogeneous essential boundary condition, (4.5)

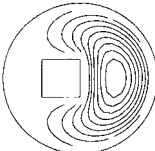
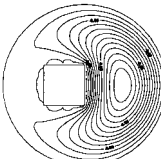
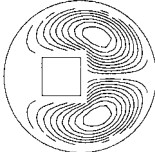
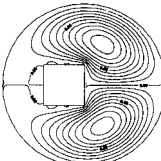
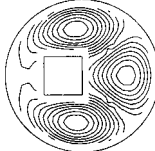
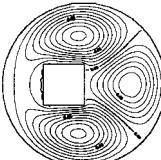

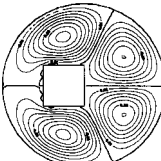

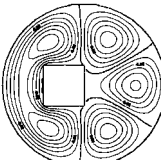
$$k_{mn} = \pi \sqrt{m^2 + n^2} \quad (m, n = 0, 1, 2, \dots),$$

homogeneous natural boundary condition. (4.6)

It is found that one of the expected spurious eigenvalue $k_{11} = 4.44$ disappeared in figure 11 for the numerical experiment. The reason may be the smaller number of boundary elements. Nevertheless, it does not matter, since all the true eigenvalues are obtained.

Case 5: inner eccentric square and outer circle (II). A multiply connected domain composed of an inner square boundary and outer circular boundary is considered, as shown in figure 13. Figure 14 also shows the minimum singular value σ_1 versus k using four approaches. The first ten eigenvalues and eigenmodes by BEM

Table 7. *The first ten eigenvalues and eigenmodes of the Helmholtz eigenvalue problem with an annular domain (II) by different approaches*

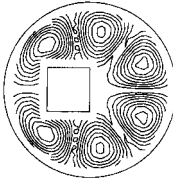
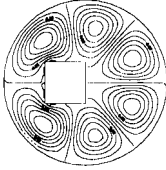
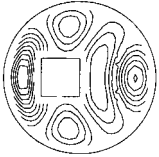
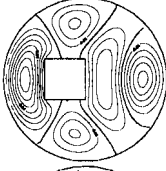
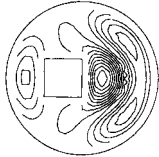
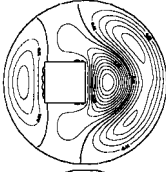
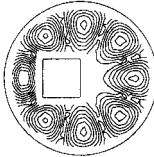
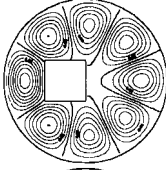

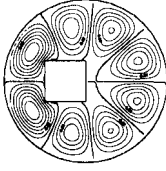
mode	eigenvalue (FEM)	mode shape (FEM)	eigenvalue (BEM)	mode shape (BEM)
1	1.81		1.81	
2	2.20		2.21	
3	2.50		2.53	
4	2.79		2.83	
5	3.07		3.10	

and FEM are shown in table 7. We expect that the positions of spurious eigenvalues are the same with equations (4.5) and (4.6). One of the expected spurious eigenvalues, $k_{11} = 4.44$, also disappeared in figure 14 for the numerical experiment.

5. Conclusions

In this paper, the mathematical analysis has shown that the spurious eigenvalues occur when either of the complex kernels $U_c(s, x)$ or $L_c(s, x)$ is used and the positions of spurious eigenvalues depend on only the shape of inner boundary for the multiply connected problem. The true and spurious eigenvalues for an annular problem were analytically studied using degenerate kernels and circulants. The mechanism of the spurious eigensolution for the multiply connected problem is similar to the fictitious frequency for the exterior problem (Chen 1998; Chen & Kuo 2000). For the multiply connected problems, the singular formulation (UT equation) results in spurious eigenvalues which are associated with the interior natural frequency with

Table 7. *Cont.*

mode	eigenvalue (FEM)	mode shape (FEM)	eigenvalue (BEM)	mode shape (BEM)
6	3.36		3.42	
7	3.40		3.47	
8	3.41		3.47	
9	3.79		3.90	
10	3.85		3.95	

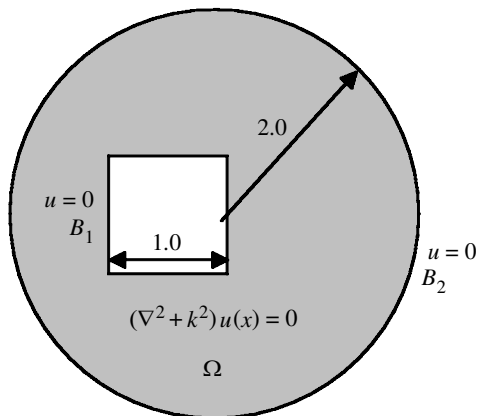


Figure 13. Helmholtz eigenvalue problem with an inner square and outer circular domain.

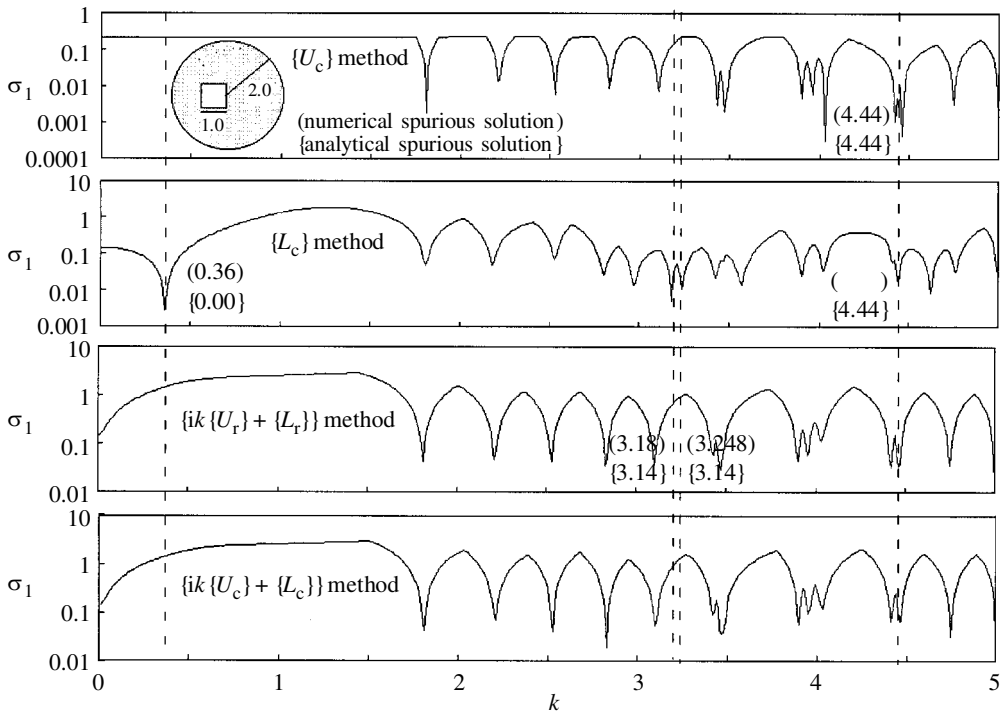


Figure 14. The minimum singular value σ_1 versus k using different approaches for the Dirichlet problem ($u = 0$) with an inner square and outer circular domain.

homogeneous essential boundary conditions, while the hypersingular formulation (LM equation) produces spurious eigenvalues which are associated with the interior eigenfrequency with homogeneous natural boundary conditions. We have employed the Burton–Miller method to filter out the spurious eigenvalues successfully and have also provided a modified Burton–Miller method to eliminate the spurious eigenvalues more efficiently. Five numerical examples were shown to demonstrate the proposed methods. The results in the numerical examples are compared with the FEM and analytical solution. Good agreement can be found.

This article originated from discussions with Dr J. R. Chang and Professor W. D. Yeih, and we are grateful to them for many suggestions. In addition, we thank Professor H.-K. Hong for his advice and guidance. Continuing support from the National Science Council, Taiwan, is also gratefully acknowledged.

References

- Burton, A. J. & Miller, G. F. 1971 The application of integral equation methods to the numerical solution of some exterior boundary-value problems. *Proc. R. Soc. Lond. A* **323**, 201–210.
- Chang, J. R. 1999 Applications of domain partitioning on vibration problems using the dual BEM. PhD thesis, Department of Harbor and River Engineering, National Taiwan Ocean University.
- Chang, J. R., Yeih, W. & Chen, J. T. 1999 Determination of natural frequencies and natural modes of a rod using the dual BEM in conjunction with the domain partition technique. *Comput. Mech.* **24**, 29–40.

- Chen, G. & Zhou, J. 1992 *Boundary element methods*. Academic.
- Chen, I. L., Chen, J. T., Kuo, S. R. & Liang, M. T. 2001 A new method for true and spurious eigensolutions of arbitrary cavities using the CHEEF method. *J. Acoust. Soc. Am.* **109**, 982–999.
- Chen, J. T. 1998 On the fictitious frequencies using dual series representation. *Mech. Res. Commun.* **25**, 529–534.
- Chen, J. T. & Hong, H. K. 1999 Review of dual boundary element methods with emphasis on hypersingular integral and divergent series. *Appl. Mech. Rev.* **52**, 17–33.
- Chen, J. T. & Kuo, S. R. 2000 On fictitious frequencies using circulants for radiation problems of a cylinder. *Mech. Res. Commun.* **27**, 49–58.
- Chen, J. T. & Wong, F. C. 1998 Dual formulation of multiple reciprocity method for the acoustic mode of a cavity with a thin partition. *J. Sound Vib.* **217**, 75–95.
- Chen, J. T., Kuo, S. R. & Huang, C. X. 1999 Analytical study and numerical experiments for true and spurious eigenvalues of a circular cavity using real part BEM. In *IUTAM/IACM/IABEM Symp. on Advanced Mathematical Computational Mechanics Aspects of Boundary Element Methods, Cracow, Poland*, pp. 18–19.
- Chen, J. T., Huang, C. X. & Wong, F. C. 2000a Determination of spurious eigenvalues and multiplicities of true eigenvalues in the dual multiple reciprocity method using the singular value decomposition technique. *J. Sound Vib.* **230**, 219–230.
- Chen, J. T., Kuo, S. R. & Cheng, Y. C. 2000b On the true and spurious eigensolutions using circulants for real-part dual BEM. *Proc. Int. Union of Theoretical of Applied Mechanics*. Kluwer.
- Davis, P. J. 1979 *Circulant matrices*. Wiley.
- De Mey, G. 1976 Calculation of the Helmholtz equation by an integral equation. *Int. J. Numer. Meth. Engng* **10**, 59–66.
- De Mey, G. 1977 A simplified integral equation method for the calculation of the eigenvalues of Helmholtz equation. *Int. J. Numer. Meth. Engng* **11**, 1340–1342.
- Gennaretti, M., Giordani, A. & Morino, L. 1977 A third-order boundary element method for exterior acoustics with applications to scattering by rigid and elastic shells. *J. Sound Vib.* **225**, 699–722.
- Goldberg, J. L. 1991 *Matrix theory with applications*. McGraw-Hill.
- Golub, G. H. & VanLoan, C. F. 1989 *Matrix computations*, 2nd edn. Baltimore, MD: The Johns Hopkins University Press.
- Hutchinson, J. R. 1985 An alternative BEM formulation applied to membrane vibrations. In *Boundary elements VII* (ed. C. A. Brebbia & G. Maier). Springer.
- Hutchinson, J. R. 1988 Vibration of plates. In *Boundary elements X* (ed. C. A. Brebbia), vol. 4, pp. 415–430. Springer.
- Hutchinson, J. R. 1991 Analysis of plates and shells by boundary collocation. In *Boundary element analysis of plates and shells* (ed. D. E. Beskos), pp. 314–368. Springer.
- Itagaki, M. & Brebbia, C. A. 1993 Source iterative multiple reciprocity technique for Helmholtz eigenvalue problems with boundary elements. In *Boundary element methods, current research in Japan and China*, pp. 79–88. *Proc. 5th Japan–China Symp. on Boundary Element Methods, Sapporo*. Elsevier.
- Itagaki, M. & Brebbia, C. A. 1994 Application of the multiple reciprocity boundary element method to neutron diffusion problems. In *The multiple reciprocity boundary element method*, ch. 6. Southampton: Computational Mechanics Publications.
- Itagaki, M., Nishiyama, S., Tomioka, S. & Enoto, T. 1997 Power iterative multiple reciprocity boundary element method for solving the three-dimensional Helmholtz equation. *Engng Analysis Bound. Elem.* **20**, 113–121.
- Kamiya, N. & Andoh, E. 1993 A note on multiple reciprocity integral formulation for Helmholtz equation. *Commun. Numer. Meth. Engng* **9**, 9–13.

- Kamiya, N., Andoh, E. & Nogae, K. 1996 A new complex-valued formulation and eigenvalue analysis of the Helmholtz equation by the boundary element method. *Adv. Engng Soft.* **26**, 219–227.
- Kuo, S. R., Chen, J. T. & Huang, C. X. 2000a Analytical study and numerical experiments for true and spurious eigensolutions of a circular cavity using the real-part dual BEM. *Int. J. Numer. Meth. Engng* **48**, 1404–1422.
- Kuo, S. R., Chen, J. T., Liou, M. L. & Chyuan, S. W. 2000b A study on the true and spurious eigenvalues for the two-dimensional Helmholtz eigenvalue problem of an annular region. *J. Chinese Inst. Civ. Hydra. Engng* **12**, 533–540. (In Chinese.)
- Kuo, S. R., Yeh, W. & Wu, Y. C. 2000c Applications of the generalized singular-value decomposition method on the eigenproblem using the incomplete boundary element formulation. *J. Sound Vib.* **235**, 813–845.
- Nowak, A. J. & Brebbia, C. A. 1989 The multiple reciprocity method—a new approach for transforming BEM domain integrals to the boundary. *Engng Analysis Bound. Elem.* **6**, 164–167.
- Nowak, A. J. & Neves, A. C. (eds) 1994 *Multiple reciprocity boundary element method*. Southampton: Computational Mechanics Publications.
- Schenck, H. A. 1968 Improved integral formulation for acoustic radiation problem. *J. Acoust. Soc. Am.* **44**, 41–58.
- Schroeder, W. & Wolff, I. 1994 The origin of spurious modes in numerical solutions of electromagnetic field eigenvalue problems. *IEEE Trans. Microwave Theory Techniques* **42**, 644–653.
- Seybert, A. F. & Rengarajan, T. K. 1968 The use of CHIEF to obtain unique solutions for acoustic radiation using boundary integral equations. *J. Acoust. Soc. Am.* **81**, 1299–1306.
- Silva, N. A. & Venturini, W. S. 1988 Dual reciprocity process applied to solve bending plate on elastic foundations. In *Boundary elements X*, vol. 3. Springer.
- Tai, G. R. G. & Shaw, R. P. 1974 Helmholtz equation eigenvalues and eigenmodes for arbitrary domains. *J. Acoust. Soc. Am.* **56**, 796–804.
- Yeh, W., Chang, J. R., Chang, C. M. & Chen, J. T. 1999a Applications of dual MRM for determining the natural frequencies and natural modes of a rod using the singular value decomposition method. *Adv. Engng Soft.* **30**, 459–468.
- Yeh, W., Chen, J. T. & Chang, C. M. 1999b Applications of dual MRM for determining the natural frequencies and natural modes of an Euler–Bernoulli beam using the singular value decomposition method. *Engng Analysis Bound. Elem.* **23**, 339–360.